Climatic and Global Validation of Daily MODIS Precipitable Water Data at AERONET Sites for Clear-sky Irradiance Modelling

Jamie M. Bright[1], Christian A. Gueymard[2], Sven Killinger[3], David Lingfors[4], Xixi Sun[5], Peng Wang[5, 6], Nicholas A. Engerer[1].

[1] Fenner School of Environment and Society, Australian National University, Canberra (Australia)

[2] Solar Consulting Services, Colebrook, NH (USA)

[3] Fraunhofer Institute for Solar Energy Systems ISE, 79100 Freiburg (Germany)

[4] Department of Engineering Sciences, Uppsala University, Uppsala (Sweden)

[5] Department of Mathematics and System Sciences, Beihang University, Beijing (China)

[6] Beijing Advanced Innovation Center for Big Data, Beihang University, Beijing (China)

Abstract

Precipitable water (PW) is an influential variable in regards to clear-sky radiation modelling and solar resource assessment. Thus, the accuracy of solar energy estimates depends on the accuracy of PW measurements. Gridded satellite information is commonly used for solar modelling because of its benefit of a broad geographical coverage, thus a global validation of commonly utilised PW products is imperative. Here, all Level-3 Moderate Resolution Imaging Spectroradiometer (MODIS) daily PW products from the Aqua and Terra satellites (at $1° \times 1°$ spatial resolution) from 01/2000 to 02/2018 are compared and validated against all of NASA's ground-sensing Aerosol Robotic NETwork (AERONET) V3 Level-2 PW daily averages from sites that have at least one year of observations during 2000–2018 (452 sites representing 675,158 observations). Furthermore, sub-categorisation by Köppen-Geiger climate regions enables climate specific validation to ascertain any distinct climatic influence. The results demonstrate significant climatological influences that impact the derived PW products. It is found that the Terra PW is more accurate than the Aqua PW, and that blending these two products yields a higher accuracy of daily PW estimates. The MODIS PW product also suffers from overestimation at larger magnitudes (>3 cm). The absolute errors do not reduce linearly with the PW magnitude, so that relative errors are far worse in areas of low PW, such as the polar climate. The equatorial climate, with the highest PW records, behaves best. Finally, a simple sensitivity test using the REST2 clear-sky radiation model shows that the global PW RMSE (0.511 cm) of the combined MODIS data would result in a 1.5-2.5% under- or overestimate on direct normal irradiance (DNI) depending on latitude relative to using the AERONET mean PW of 1.8971 cm. It is thus concluded that the daily MODIS PW product is not ideal for clear-sky radiation modelling, at least whenever accurate DNI predictions are necessary on a global scale.

Keywords: MODIS, AERONET, clear-sky model, precipitable water, aerosol optical depth, global validation.

1. Introduction

Precipitable water (PW) is the atmospheric variable that quantifies the depth (typically expressed in cm) of water vapour present within a column of atmosphere, should all the water vapour be precipitated as liquid water. Water vapour is the most important gaseous element of infrared opacity in the atmosphere and leads to significant attenuation of radiation (Gueymard, 2014a). In turn, PW is a convenient way to quantify the water vapour amount within the atmosphere at any instant (Pérez-Ramírez et al., 2014). Clear-sky radiation modelling is fundamental to all solar forecasting estimates and historical database production (Engerer et al., 2017). Many different clear-sky radiation models have been validated around the world in various studies (Sun et al., 2018; Ineichen, 2016; Engerer and Mills, 2015; Gueymard, 1993, 2012a). In such studies, the most successful models were those that use a specific representation of PW within their derivation. Some simpler radiation models consider the PW attenuation only indirectly through the Linke turbidity factor, which combines the PW effect with those of aerosols and air mass. Of the 57 clear-sky models analysed by Sun et al. (2018), for instance, 52 models have specific consideration for PW. The 5 models that do not consider PW are at least 30-year old and tend to underperform. Global coverage of PW is of significant importance in solar applications such as satellite-based forecasting and historical reconstructions of solar irradiance time series. It is now possible to use reanalysis data, such as NASA's MERRA2, ECMWF's CAMS, or NOAA's NCEP, whereby global high-resolution derivations of PW are offered. However, these reanalyses are also more or less strongly dependent on the raw estimates from satellite sensors that are assimilated into the atmospheric model to constrain the boundary conditions. It is, therefore, imperative to have a fundamental

Selection and/or peer review under responsibility of Scientific Committee
doi:10.18086/eurosun2018.09.07 Available at http://proceedings.ises.org

understanding of how accurate the original satellite-based estimates are, and to ascertain whether specific climatological biases might exist.

The satellite observations/retrievals from the two MODIS (Moderate Resolution Imaging Spectroradiometer) sensors across the two satellite platforms of Aqua (launched 2002) and Terra (launched 1999) are of particular interest because they were specifically designed to monitor various atmospheric constituents of Earth. Furthermore, the MODIS products offer gridded access at 10 km x 10 km spatial resolution globally, of which a quality-controlled product is available at a daily temporal scale. This type of gridded data is particularly useful for applications such as solar forecasting and worldwide irradiance estimates (Engerer et al., 2017). The PW products from the two MODIS platforms have been validated in a few studies at various spatial or temporal scales. The spatial scale, in particular, can be as small as one or more specific ground sites (Gui et al., 2017; Li et al., 2003; Lu et al., 2011), a region (Kang et al., 2016; Kumar et al., 2013; Liu et al., 2006; Wang et al., 2017), or as large as a country or subcontinent (Bennouna et al., 2013; Prasad et al., 2009; Roman et al., 2014; Shi et al., 2018; Vaquero-Martinez et al., 2018; Wong et al., 2014). The results of these studies generally showed good agreement between the PW data from MODIS and from other experimental sources. There are only a few known studies whereby the MODIS PW data sources are used as input to solar radiation models to test the effect of any potential error propagation on modelled surface irradiance. While observing a strong agreement between reanalysis data and other PW determinations (although not from MODIS) in a case study, Gueymard (2014a) observed that errors in PW did not result in significant errors in modelled clear-sky direct or global irradiance. In a more detailed study, Roman et al. (2014) evaluated the uncertainty of MODIS PW data against observations from six ground-based stations located in Spain, and the resulting uncertainty on modelled global irradiance. This was found reasonable, but not negligible (less than 4% for solar zenith angles below 75°).

Based on this literature review, there is considerable scope to offer deeper insight into the accuracy assessment of MODIS PW in terms of its performance at the largest (global) scale, possible geographic variations of this performance, and the resulting impact on modelled solar irradiance at the surface. The geographic influence of PW is explored here using climate categorisation. In parallel, it is worthwhile to compare the MODIS PW products from the two platforms, Aqua and Terra. Certain products from these platforms have been compared to each other and to ground truth previously, noting distinct discrepancies between them, in part caused by a more rapid degradation of the MODIS-Terra instrument (Levy et al., 2018).

The Aerosol Robotic Network (AERONET; http://aeronet.gsfc.nasa.gov/) offers ground truth of PW, as measured with an automatic sunphotometer in the 940-nm absorption band. AERONET PW is measured at sites in various kinds of climate and environment around the world. There are many research studies whereby a MODIS product (most usually AOD) is compared to its AERONET counterpart for analysis of a distinct climatic zone (Shi et al., 2018; Zhong et al., 2015), often accompanied by a correction factor that is specific to those individual sites analysed. There are only a few research studies focusing on comparing Level-3 MODIS AOD against ground AERONET stations. One such study by Ruiz-Arias et al. (2013) evaluated the performance of the Level-3 MODIS AOD both globally and by geographic region (e.g., Australia, Southern Africa, and Northwest America); they demonstrated distinct errors by region and suitability for solar radiation calculations in numerical weather modelling. This level of analysis previously performed on AOD can be extended to the PW product, which is the major objective of the present investigation. In that respect, the global validation of the latest version (Collection 6.1) of MODIS Aqua and Terra Level-3 satellite-derived PW is performed by comparing its daily values to daily-mean measurements from AERONET. One goal here is to assess performance of such data similarly to the regional analysis of Ruiz-Arias et al. (2013). One important new feature developed here, however, is the subcategorisation of the AERONET sites into different statistically distinguishable climatic regions. This is achieved following the Köppen-Geiger climate classification (Kottek et al., 2006), as explained further in Section 2. Additional goals are (i) to ascertain whether blending the datasets from the two MODIS platforms can improve the PW retrievals; and (ii) to establish whether or not the accuracy of the MODIS PW data is sufficient to guarantee solar irradiance predictions with the low uncertainty required by demanding solar resource assessments.

2. Data

PW is retrieved from the MODIS instrument aboard the Terra (EOS AM; MOD08_D3 product) and Aqua (EOS PM; MYD08_D3 product) satellites. Only the Level-3 daily products at 1x1° spatial resolution are considered here. All MODIS data records from 01/2000 to 02/2018 are used here, as offered by the Collection 6.1 database. This is available from NASA's Level-3 and Atmosphere Archive & Distribution System (LAADS) Distributed Active Archive Center (DAAC) (https://ladsweb.nascom.nasa.gov).

PW is independently measured by multiple AERONET sites around the world with extensive global coverage (Dubovik et al. 2002; Eck et al. 2003; Holben et al. 1998; Sinyuk et al. 2012). The daily averages are obtained from the V3 collection that has Level-2 quality assurance, which means that both pre- and post-field calibration are already applied, that the data time series is manually inspected for consistency, and that it is screened to remove cloud interference. Only sites with more than a combined 365 daily values during 01/2000 to 02/2018 with coincident MODIS data are considered, totalling 452 AERONET sites. The total number of validation data points available for PW comparison is 675,158 daily observations.

The Köppen-Geiger classification has five main classes that are denoted A, B, C, D and E, respectively representing equatorial, arid, warm temperate, snow, and polar climates (Fig. 1). Further complexity exists with up to 29 variations derived from the five main classifiers. This more detailed classification is not considered here because it would significantly reduce the sample size within each class. The latitude and longitude boundaries of each climate class are provided in lookup tables (Kottek et al., 2006).

Gueymard and Thevenard (2009) expressed the general need for altitude corrections to gridded data due to the natural decrease of PW with increasing altitude (due to its impact on temperature and pressure profiles). This is particularly significant when the satellite pixel's mean elevation differs from the ground validation site's elevation, for example over mountainous areas. Fig. 2 illustrates the differences of the reported altitude at station height to the gridded digital surface elevations from MODIS. The proposed correction is based on a scale-height approximation:

$$PW(h) = PW(h_0) \times \exp\left[\frac{h_0 - h}{H_w}\right], \qquad \text{(eq. 1)}$$

where h_0 is the reference site's satellite pixel elevation above mean sea level (amsl), and h is the AERONET-defined elevation of the site. The water vapour scale height H_w is experimentally derived (Hayasaka et al., 2007) and varies both spatially and temporarily. Because there has been little global study to estimate the scale height and its variability, Gueymard and Thevenard (2009) proposed a mean value of $H_w = 2100$ m, which is assumed satisfactory for general global purpose. Using all possible pairs of MODIS pixels and AERONET sites, the correction factor $f = \exp[(h_0 - h)/H_w] = PW(h)/PW(h_0)$ is found to vary between a minimum of 0.303 and a maximum of 2.177, with a mean of 1.13. All sites' f values are reasonably well represented by a Burr distribution $B(\alpha, c, k)$, where α, c and k are the scale, first shape and second shape parameters with values of ≈0.988, 32.3, and 0.672, respectively. A scatter plot of this correction value versus the RMSE of MODIS combined PW to AERONET PW is presented later in Fig. 5 (bottom right).

3. Methodology

AERONET sites are first subcategorised into the five climate classes mentioned above and shown in Fig. 1. The global performance of the MODIS products is simply calculated as an equally-weighted mean of the error metrics derived for each climate class. This way, a climate class having a large number of sites (the majority of AERONET sites are warm temperate) has the same weight than a class with fewer sites. Hence, a highly populated class cannot overwhelm the overall results. MODIS L3 daily PW values are extracted from the appropriate gridded location that correspond to each AERONET site and for all days with valid data. MODIS PW is corrected for natural variations in water vapour caused by height differences, according to Eq. 1.

Error metrics are then derived for each of the five climate classifications. The error metrics used here are the root mean square error (RMSE), the mean bias error (MBE), the mean absolute error (MAE), and the Pearson correlation coefficient (R). Relative metrics (rRMSE and rMBE) are also evaluated, after normalisation by their respective mean. Absolute metrics are possibly important because the impact of PW on the modelled surface irradiance is larger when PW is small (Gueymard, 2014a). The interest of also using relative metrics in this case is to help compare different climate regions on a relatively equal footing. Because PW in equatorial regions is typically higher than in polar climates, it is important to have a normalised approach to make the metrics comparable. The effectiveness of this principle is demonstrated in Section 4. It is useful to have an established target of performance in order to ascertain whether or not the MODIS PW retrievals perform satisfactorily. Further complexity could be added, such as the statistical performance indicators suggested by Gueymard (2014b), but this is deemed unnecessary at this stage.

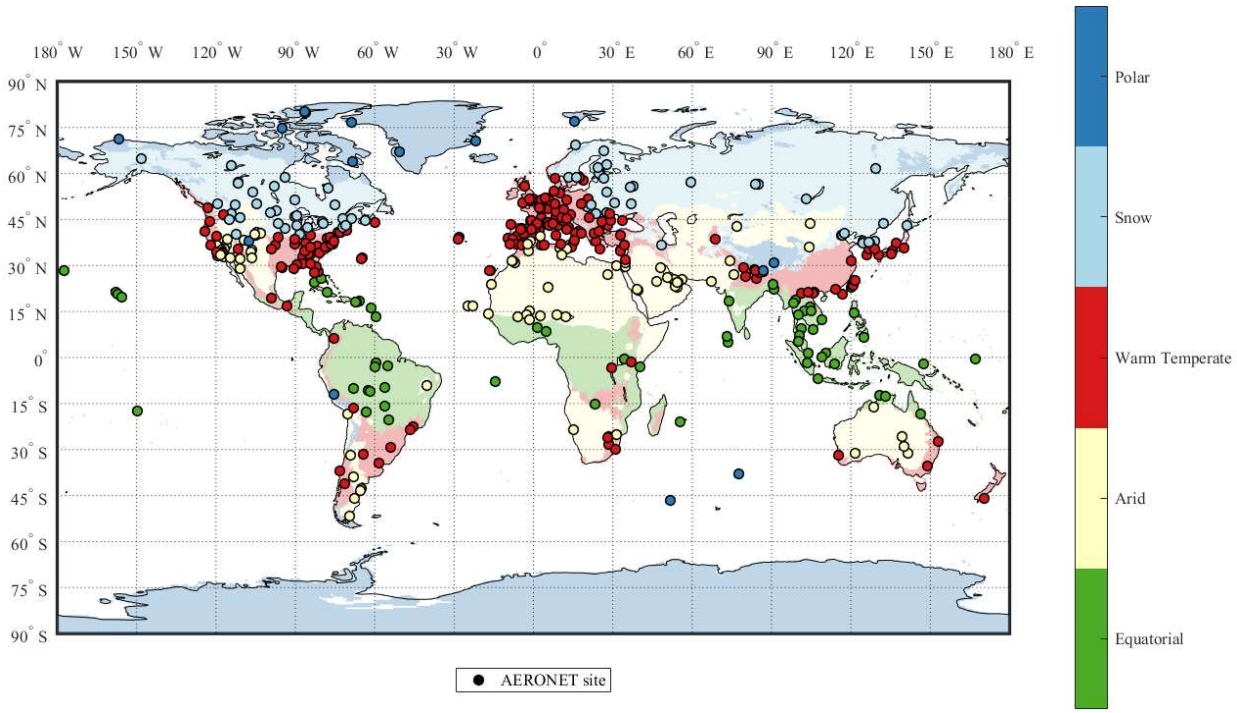

Fig. 1: Equidistant cylindrical projected world map indicating the location of the 452 AERONET sites considered within this study. Each AERONET site is coloured according to its associated Köppen-Geiger climate classification, as indicated by the colour bar.

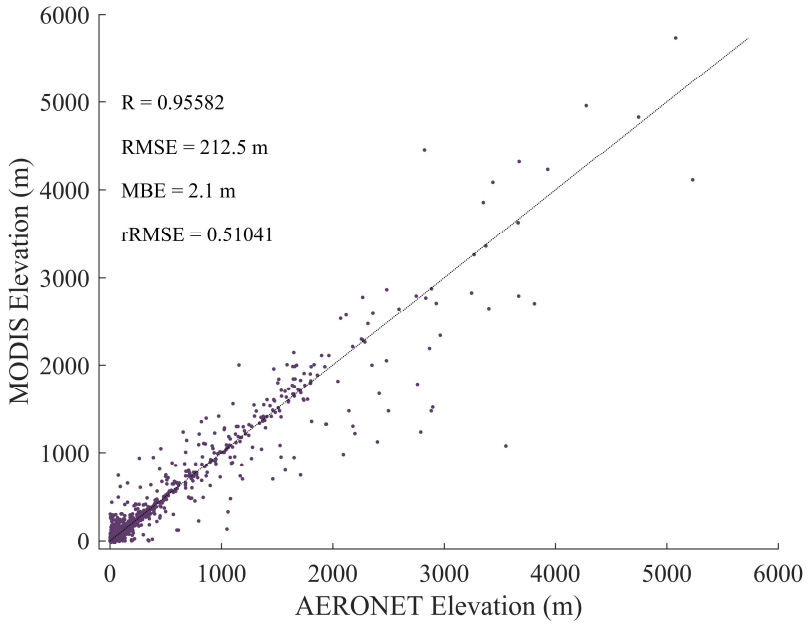

Fig. 2: Observed differences between reported AERONET station heights (h) used within the study and the gridded surface elevation from the MODIS platform data (h_0). These discrepancies are attributed to terrain changes within the 10 km² MODIS pixels.

In order to test the influence of PW on clear-sky radiation modelling, a top-performing model—REST2v5, as detailed by Gueymard (2008)—is selected based on the thorough study from Sun et al. (2018). REST2v5 was shown to perform excellently across all Köppen-Geiger climate classifications and is therefore considered a suitable test bed to explore the influence of PW on irradiance. A simple test is done here in a pseudo-random way by selecting the mean annual irradiance outputs from REST2v5 obtained at midday for 10 locations of constant 0° longitude and latitudes increasing from 0° to 90° with 10° increments. All input variables are fixed except PW, which is explored across its full range. The REST2 model requires a number of input variables besides PW; here they are imposed the following default values: pressure = 1013.25 mb, total column ozone = 0.35 atm-cm, total column nitrogen dioxide = 0.0002 atm-cm, Ångström exponent = 1.3, Ångström turbidity = 0.2 and surface albedo = 0.3. PW is varied parametrically from 0 to 10 cm in 0.05-cm increments to observe the effect of varying PW on the mean annual midday irradiance at different points on the surface of the Earth, and subsequently estimate the impact of the MODIS PW errors on the modelled irradiance uncertainty.

4. Results and discussion

In addition to the normal PW products from MODIS Aqua and Terra, a third product (referred to here as "combined platform") is obtained as an equal blend, using the mean value when both Aqua and Terra data are available. The performance of these three products is obtained by comparison with the AERONET PW ground data, all within each of the five climate classes defined above. A "global climate" category, which encompasses all five classes and thus all AERONET stations, is also considered. Performance metrics are thus evaluated for three MODIS platforms (Aqua, Terra and Combined), each across six climate regions (5 Koppen classes + global), i.e., 18 cases total. To conform with the goals of this study, the discussion will revolve around observable differences between climate regions for each of the MODIS PW platforms, as well as comparisons between the Aqua and Terra platforms to detect any systematic bias or climate-induced differences between them.

All the error metrics for each climate region and variable are presented in Tab. 1. The table is colour coded for better legibility, considering the disaggregation by climate region. Furthermore, boldface is used to indicate the best performing platform for each of the presented metrics. For example, *R* is found to be highest in all cases when the Aqua and Terra data are averaged to create the combined data source, which is why the combined value for *R* is in boldface.

It is remarkable that the lowest RMSE, rRMSE and MAE, as well as the highest *R* is nearly always best for the "MODIS combination" data source. The combined rRMSE is outperformed by the Terra platform in only one specific case—the equatorial climate class. These results are in stark contrast to those for MBE and rMBE, where Terra always outperforms the other data sources. It is evident that the Aqua platform has the worst bias, overestimating consistently in all climates. Because of this significant Aqua bias, the combination of Aqua and Terra cannot outperform the less biased Terra platform. Interestingly, both Aqua and Terra platforms (and therefore also their combination) overestimate in every climate.

Tab. 1: Error metrics of climate-specific and global performance of PW from MODIS Aqua, MODIS Terra and their combination (mean of Aqua and Terra). Climate regions are highlighted by colour. The best performing platforms are highlighted in boldface.

Platform	RMSE (cm)	rRMSE	MBE (cm)	rMBE	MAE (cm)	R	Climate
Aqua	0.922	0.272	-0.587	-0.172	0.748	0.794	Equatorial
Terra	**0.681**	**0.205**	**-0.199**	**-0.066**	**0.545**	0.774	
Combined	0.709	0.216	-0.376	-0.116	0.576	**0.817**	
Aqua	0.576	0.392	-0.269	-0.197	0.441	0.832	Arid
Terra	0.577	0.398	**-0.234**	**-0.175**	0.442	0.813	
Combined	**0.536**	**0.373**	-0.244	-0.186	**0.418**	**0.845**	
Aqua	0.608	0.403	-0.302	-0.232	0.471	0.846	Warm Temperate
Terra	0.517	0.357	**-0.092**	**-0.117**	0.399	0.840	
Combined	**0.504**	**0.349**	-0.186	-0.170	**0.394**	**0.864**	
Aqua	0.495	0.393	-0.250	-0.203	0.362	0.884	Snow
Terra	0.406	0.335	**-0.107**	**-0.100**	0.298	0.881	
Combined	**0.401**	**0.329**	-0.171	-0.147	**0.297**	**0.903**	
Aqua	0.436	0.955	-0.245	-0.648	0.336	0.823	Polar
Terra	0.424	0.947	**-0.220**	**-0.629**	0.326	0.833	
Combined	**0.404**	**0.903**	-0.233	-0.635	**0.319**	**0.857**	
Aqua	0.607	0.483	-0.331	-0.290	0.471	0.836	Global
Terra	0.521	0.448	**-0.170**	**-0.218**	0.402	0.828	
Combined	**0.511**	**0.434**	-0.242	-0.251	**0.401**	**0.857**	

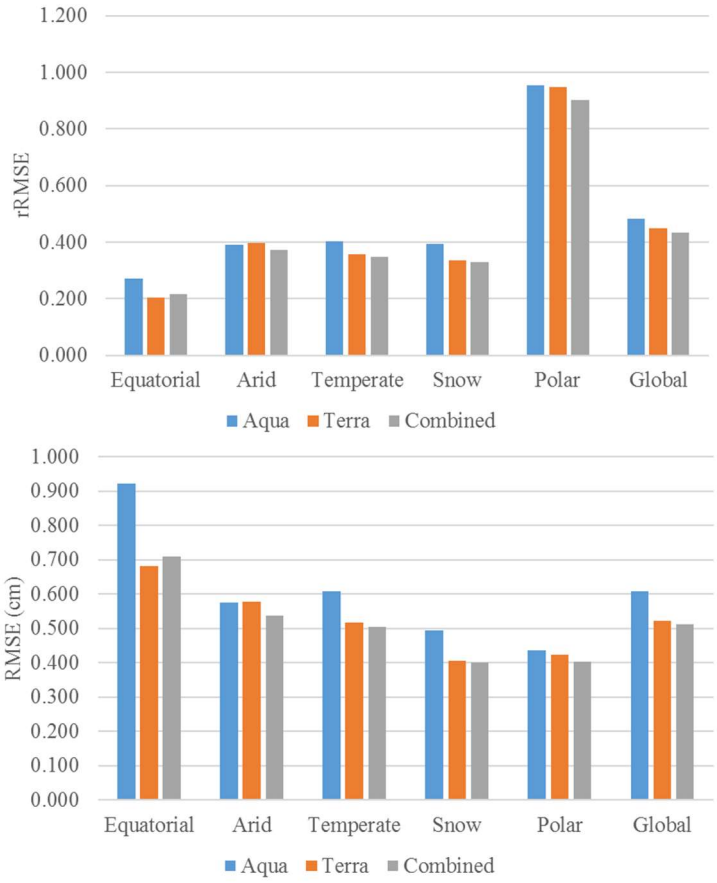

Fig. 3: Bar graph representation of the PW (top) relative RMSE, and (bottom) absolute RMSE (cm). The coloured series represent the three different platforms of MODIS Aqua, MODIS Terra and MODIS combination.

This lends weight to previous arguments (e.g. Shi et al., 2018) that a flat bias correction could be applied, whether on a climate specific scale or globally. The polar PW bias is particularly strong, suggesting the necessity of some bias correction there. These conclusions, however, are based on the assumption that the AERONET PW is itself unbiased in any climate region, and represents "ground truth" for satellite data, exactly as the AERONET AOD product.

RMSEs from Tab. 1 are graphically represented as bar plots in Fig. 3, relative to both the relative (top) and absolute (bottom) definitions. These two metrics (RMSE and rRMSE) are selected to provide a good indication of overall performance of each platform. PW displays the largest relative errors under polar conditions, where it is low. Naturally, the global-climate performance cannot exceed the performance of PW under any climate class since it is obtained as the mean performance of all climates. Conversely, the equatorial climate (where PW is high) performs best for all platforms. For a better understanding of how these metrics relate to the data, scatter plots of PW in each climate are plotted for the combined Aqua and Terra platforms in Fig. 4. The combined data source is selected here because it offers the best results. The scatter plots corroborate the poor polar rRMSE results shown in Fig. 3 (top).

Fig. 3 (bottom) displays the absolute RMSE and shows a different behaviour than rRMSE. Whilst relative metrics are useful to compare how good the performance of MODIS is relatively to each climate, they do not truly illustrate the actual capability of the MODIS methodology itself. The *relative* performance of PW is found best in equatorial regions, but simultaneously, and counterintuitively, the absolute error in those regions is the worst in almost all cases. The climatic regions generally follow a latitudinal relationship (albeit with altitude exceptions) that can be observed in Fig. 1; from Fig. 3 (bottom) it is clear that the PW RMSE decreases with latitude. A possible explanation is that satellite parallax corrections influence the quality of the retrievals.

The RMSE is almost always improved by combining Aqua and Terra, with the notable exception of the equatorial climate where Terra performs best. The "global" classification can be considered as the overall performance of combined MODIS Aqua and Terra as it is the mean of all other climates. In terms of absolute RMSE, the global performance of their combination is 0.511 cm, compared to a mean AERONET value from all 452 sites of 1.897 cm. Typically, relative errors are larger at sites where typical PW values are low, since the MODIS retrieval algorithms are then closer to their detection limit (Ruiz-Arias et al., 2013).

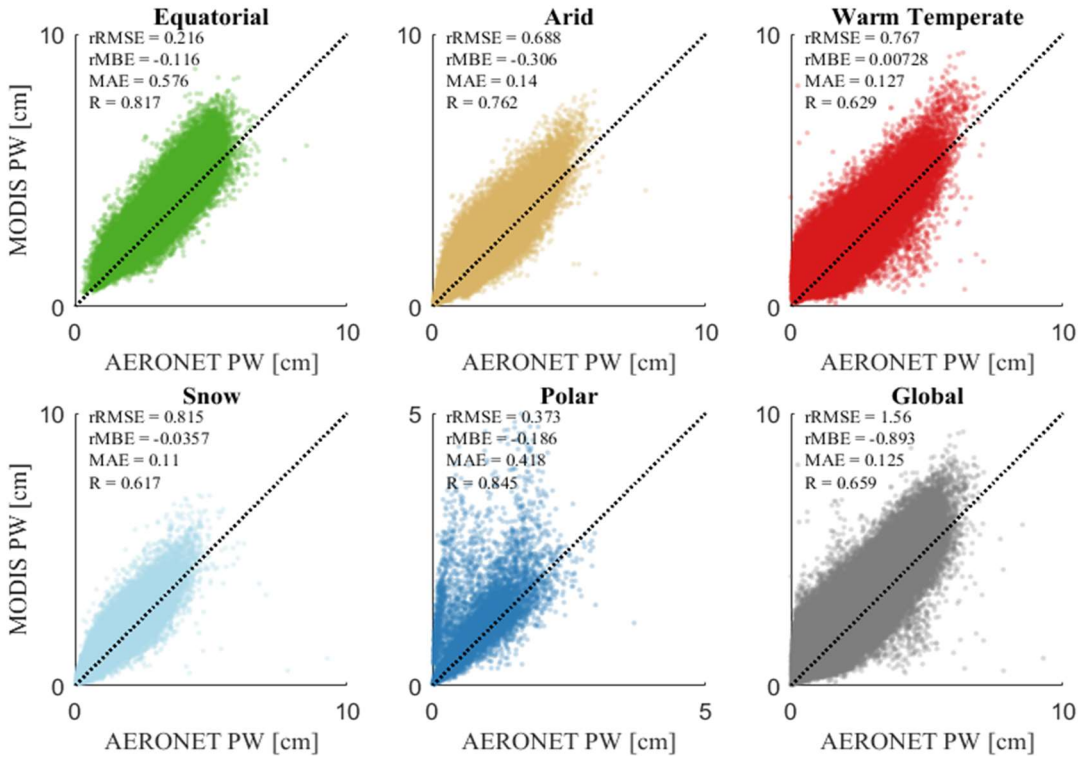

Fig. 4: Scatter plots of the combined MODIS Aqua and Terra PW product against AERONET ground measurements in each climate zone, as well as the global climate zone. A diagonal is plotted to indicate perfect performance. The polar climate has different axes limits, for legibility. The rRMSE, rMBE, MAE and *R* metrics are stated in each panel. Scatter point transparency is in place so that darker regions represent a greater density of data.

Fig. 5 analyses all the daily PW data from Aqua and Terra against AERONET ground stations, as well as against each other. A distinctive overestimation occurs when PW increases above ≈3 cm, particularly in the case of Aqua. However, the linear correlation is high for Aqua and Terra (R=0.836 and 0.828, respectively). Some sites do not match the linear fit, even after scale-height correction, which was not expected. For instance, consider the two red circles highlighting significant overestimations made by MODIS. From Fig. 4, most of these sites appear to be in the polar climate, although some warm temperate regions demonstrate similar behaviour. The bottom-left plot in Fig. 5 displays a good agreement between Aqua and Terra platforms with, however, significant scatter and larger Aqua values in general. Both platforms are seemingly in agreement for the potentially "erroneous" data circled in the two upper plots. These features highlighted in the circles do not appear when directly comparing Aqua to Terra directly because they are then closer to the diagonal. This suggests that both Aqua and Terra significantly underestimate at the same locations. The bottom-right plot tests the potential for introducing error from scale height correction, since the proposed correction was only previously tested on monthly data. We observe no correlation for both Aqua and Terra scale height correction to the observed, site-specific RMSE. We do observe that the second largest RMSE does coincide with the largest correction factor, perhaps suggesting an error in station height reporting. From data exploration, we observed no globally applicable rule that elevation is the cause of error for PW despite the fact that 8 of the 10 worst performing sites are situated at high (>2 km) elevation.

To evaluate the influence of PW on clear-sky surface irradiance, a simple test is performed using the REST2 clear-sky radiation model (Gueymard, 2008), as described in Section 3. Multiple latitudes of the north hemisphere are tested at a fixed longitude of 0°. Fig. 6 illustrates the change in mean annual midday clear-sky irradiances of the global horizontal irradiance (GHI), direct normal irradiance (DNI) and diffuse horizontal irradiance (DHI) when fixing all input variables while varying PW. As expected, DNI is the most impacted by PW. The sensitivity of DNI to PW is stronger for PW between 0 and 5 cm, and less in the range 5–10 cm, thus corroborating previous results (Gueymard, 2014a). In comparison with Figs. 4 and 5, it is clear that the vast majority of PW daily values are within the range of 0–5 cm, hence any error in that interval may result in significant deviations in the modelled irradiances. The irradiance reduction with increasing PW with reference to the ideal case when PW=0 is illustrated in Fig. 7.

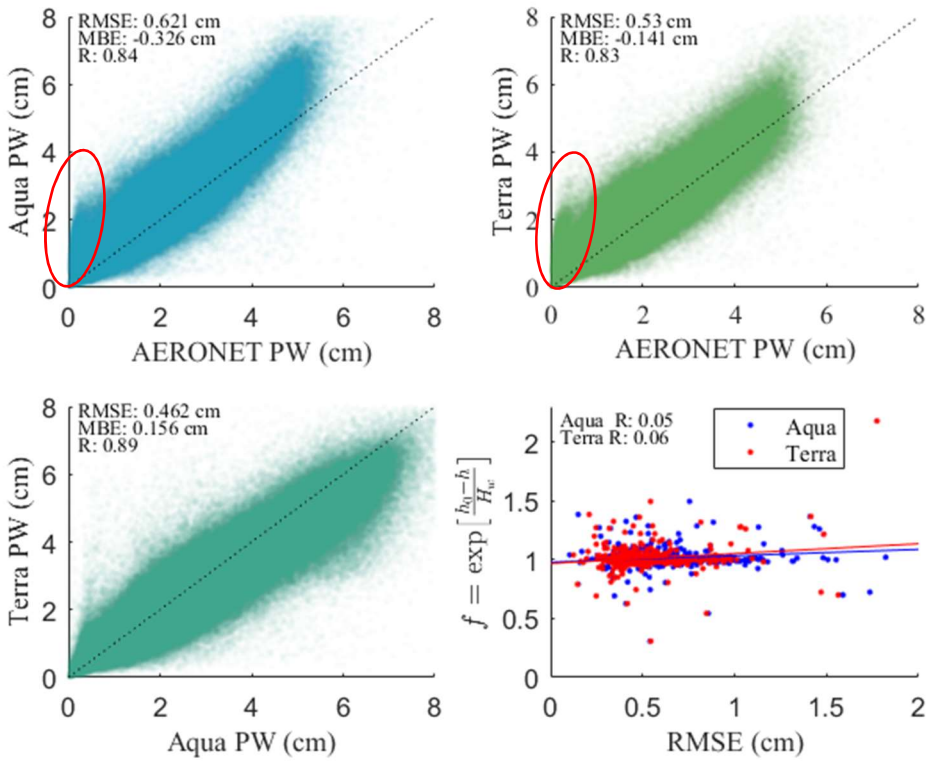

Fig. 5. (Top left) Aqua PW product plotted against AERONET PW for all 452 sites with rRMSE, rMBE and *R* indicated. (Top right) As before but for Terra. (Bottom left) Terra PW plotted against Aqua PW with error metrics. (Bottom right) Aqua and Terra PW RMSE against site elevation. A linear fit is applied and the corresponding Pearson correlation indicated for both Aqua and Terra.

The gradient is illustrative of the sensitivity of the modelled irradiance to errors in the PW input. Were we to set PW to the mean AERONET value of 1.897 cm, and apply a 0.511 cm underestimate and overestimate, the increase and decrease in GHI, DHI and DNI can be significant. These are presented in Fig. 8 where we observe typical variance of 14 Wm^{-2} overestimation in GHI when PW is underestimated by 0.511 cm, and 12 Wm^{-2} underestimation in GHI when PW is overestimated by 0.511cm at a latitude of 0 degrees. The relative error impact on GHI increases with latitude from 1.25 to 1.75% of GHI. The DNI is more sensitive to changes in PW than the DHI. One must remember that these are distinct cases represented by the global RMSE versus the global average PW. The impact on GHI can be considerably worse with the persistence of larger errors. Looking back to the top row in Fig. 5, we observe many instances where the estimated MODIS PW are regularly 3cm over estimated, which could result in a reduction in DNI by up to 100 Wm^{-2}, this does of course depend on the actual magnitude of the PW at the time.

What is most significant about Figs. 6 and 7 is that the extreme latitudes (towards $\pm 90°$), despite having reduced absolute magnitude of irradiance, have the most significant relative variability in PW. This is primarily due to the preponderance of large air masses (low sun), and therefore increased interaction of sunlight with water vapour.

Since Fig. 3 showed that the relative error in PW is the highest over polar regions, it can be inferred that small absolute errors around the typical polar PW values (≈1.5 cm or less) will result in significant impact on the modelled clear-sky irradiance. Hence, the global RMSE of 0.5 cm appears inadequate for accurate clear-sky irradiance modelling, particularly in climates of reduced PW (e.g., polar regions). Over warmer regions, such as at temperate or equatorial latitudes, the MODIS PW data sources appear more satisfactory in general, thus yielding reasonable accuracy in modelled irradiance and confirming previous results (Gueymard, 2014a; Roman et al., 2014).

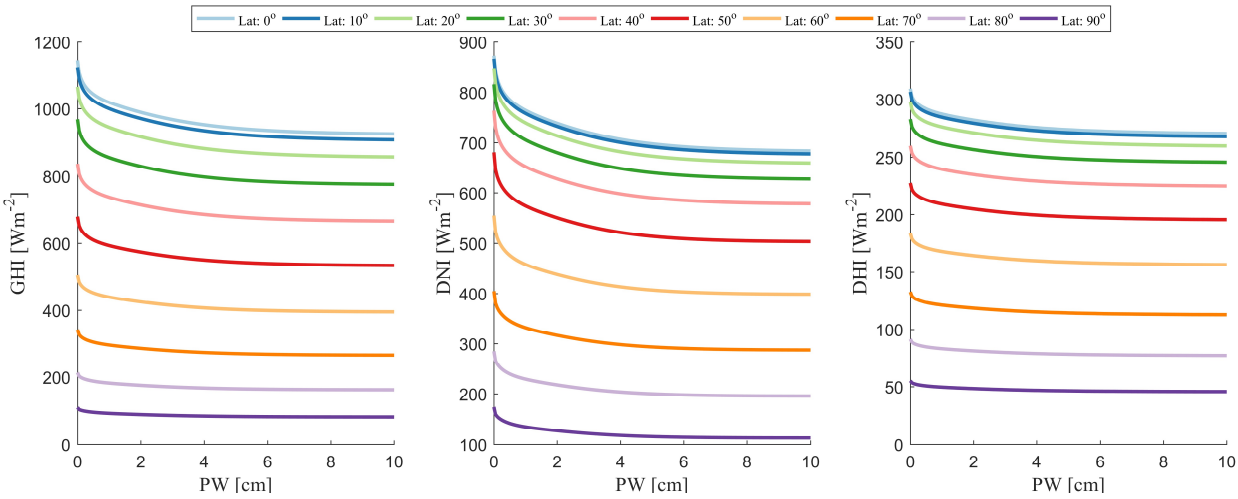

Fig. 6: Mean annual midday clear-sky global horizontal, direct normal and diffuse horizontal irradiance at latitudes ranging from 0° to 90° with 10° increments and fixed longitude of 0° as calculated from the REST2 clear-sky model (Gueymard, 2008) using constants of pressure = 1013.25 mb, total column ozone = 0.35 atm-cm, total column nitrogen dioxide = 0.0002 atm-cm, Ångström exponent = 1.3, Ångström turbidity = 0.2 and surface albedo = 0.3. The PW is varied from 0 to 10 atm-cm with 0.05 increments. Note the difference in scales on the y-axes.

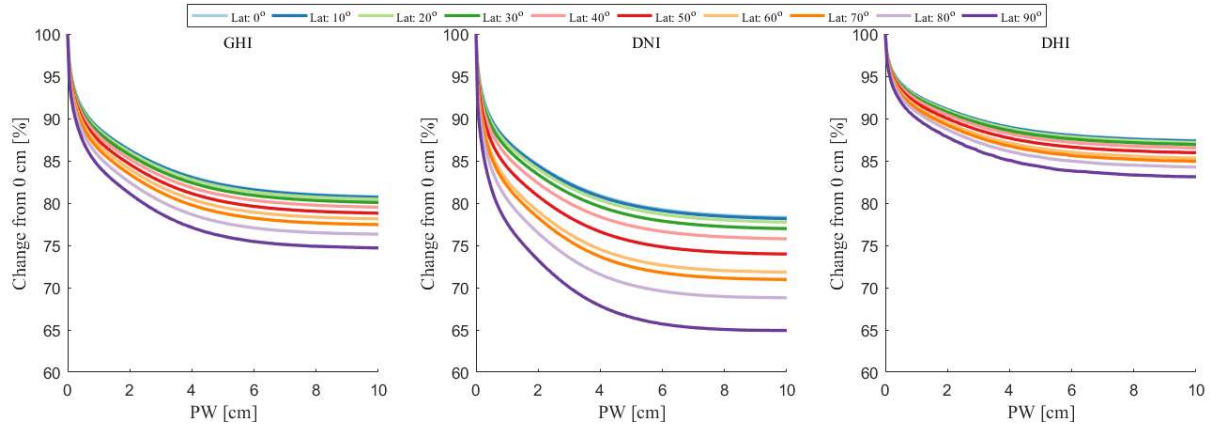

Fig. 7: Percentage reduction of mean annual midday global clear-sky global horizontal, direct normal and diffuse horizontal irradiance expressed in relation to the irradiance at PW=0 cm at latitudes ranging from 0° to 90° with 10° increments and fixed longitude of 0° as calculated from the REST2 clear-sky model (Gueymard, 2008) using constants of pressure = 1013.25 mb, total column ozone = 0.35 atm-cm, total column nitrogen dioxide = 0.0002 atm-cm, Ångström exponent = 1.3, Ångström turbidity = 0.2 and surface albedo = 0.3.

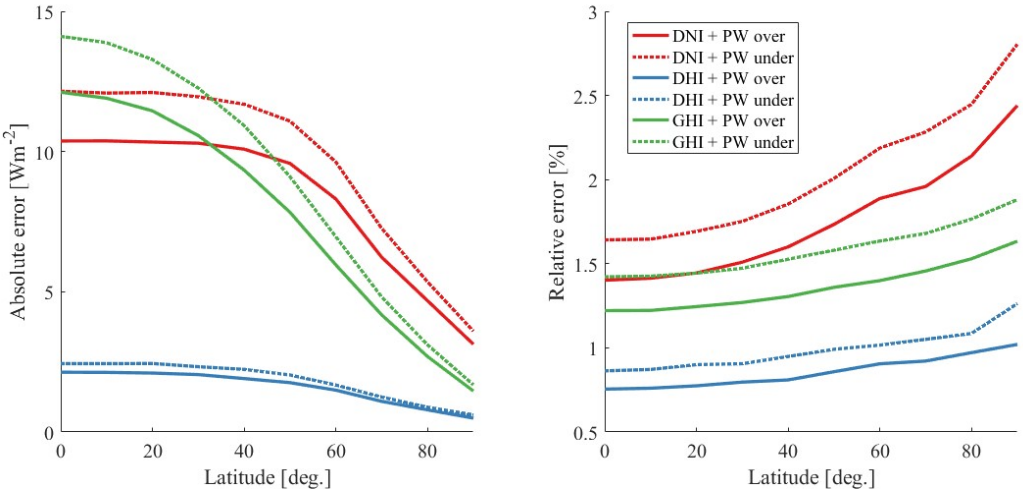

Fig. 8: The absolute difference (left) and relative (right) difference in irradiance at different latitudes when compared to the irradiance derived with the mean AERONET PW of 1.8971 cm. PW over and under represents overestimate and underestimate by 0.511 cm, which is the global PW RMSE.

5. Conclusions

Precipitable Water (PW) is an important atmospheric variable that directly impacts the accuracy of clear-sky irradiance modelled estimates around the world. Access to gridded PW is only available from reanalysis databases or from satellites such as the MODIS (Moderate Resolution Imaging Spectroradiometer) instrument on board the polar orbiting pair of the Aqua and Terra platforms. As the reanalysis generally depend on satellite measurements, it is important that the accuracy of satellite PW products be validated against high-quality ground data, such as those from the worldwide AERONET network. In this study, all AERONET sites with at least 365 days of data (452 sites) were considered to validate the MODIS products.

This paper analysed all data from the MODIS Aqua and Terra PW products from the beginning of operations (2002 for Aqua and 2000 for Terra) to 02/2018. These daily datasets were validated against the ground truth from 452 AERONET sites. The total number of PW validation data points available was 675,158. An added complexity was introduced by categorising each AERONET site into its associated Köppen-Geiger climate classification, defined as equatorial, arid, warm temperate, snow and polar. A global climate classification was also established by taking an equal average of the results from all five root climates. The MODIS Aqua and Terra platforms were validated, as well as an equal blend of both Aqua and Terra measurements called the "combined platform".

This combined platform offered the most consistently low errors across all climates and globally in terms of both relative and absolute RMSE, MAE and best performing R. It is, therefore, concluded that the most appropriate values of daily MODIS PW is from this equal blend of Aqua and Terra data. Estimations of PW were found to perform the worst in the polar climate, despite having a low RMSE when compared to other climates. Because typical polar values of PW are much smaller than elsewhere, while the retrieval error is not negligible, the relative performance is considerably weaker. This is perhaps due to the adverse conditions in polar areas with considerable and regular cloud cover periods that may interfere with observation measurements, or to the adverse impact of a high surface albedo, whose large signal can overwhelm the relatively small signal of the MODIS scanner. The Aqua platform overestimates PW more so than the Terra platform, which also overestimates PW. The Terra PW generally performs better than Aqua, though never as good as the combined platform. This may be caused by the different flight path timings of the two platforms, and any morning/afternoon asymmetry in the natural daily PW patterns, which is perhaps offset through blending.

The REST2 clear-sky irradiance model was tested for its sensitivity to PW. Low PW values are most sensitive to errors. Hence, the high rRMSE and generally poor RMSE of the PW daily MODIS products are poorly suited to clear-sky modelling in overall low PW areas, at least without local or global bias correction. We present the impact of typical sensitivity to the global RMSE of combined MODIS PW and see typical and persistent over- and underestimates of between 1-2% in GHI, though observe individual instances of up to 15% underestimation in DNI. Subsequent studies are needed to evaluate whether alternative gridded databases, from other satellites or reanalysis products, would be more appropriate.

6. Acknowledgements

The authors would like to thank the Australian Renewable Energy Agency (ARENA) for partially supporting this work (Research and Development Programme Funding: G00854 — Real-time Operational Distributed PV Simulations for Distribution Network Service Providers).

The Principal Investigator and staff of each of the 452 AERONET sites used in this investigation are warmly thanked for establishing and maintaining this invaluable source of data.

7. References

Bennouna, Y.S., Torres, B., Cachorro, V.E., Ortiz de Galisteoa, J.P., Toledanoa, C. 2013. The evaluation of the integrated water vapour annual cycle over the Iberian Peninsula from EOS-MODIS against different ground-based techniques. Q. J. R. Meteorol. Soc. 139. 1935–1956.

Chu, D.A. et al. 2002. Validation of MODIS aerosol optical depth retrieval over land. Geophys. Res. Lett. 29.

Chung, C.E. et al. 2005, Global anthropogenic aerosol direct forcing derived from satellite and ground-based observations. J. Geophys Res. 110D. doi:10/1029/2005JD006356.

Dubovik, O., Holben, B.N., Eck, T.F., Smirnov, A., Kaufman, Y.J., King, M.D., Tanre, D., Slutsker, I., 2002. Vari-

ability of absorption and optical properties of key aerosol types observed in worldwide locations. J.Atm.Sci., 59, 590-608.

Eck, T.F., Holben, B.N., Reid, J.S., O'Neill, N.T., Schafer, J.S., Dubovik, O., Smirnov, A., Yamasoe, M.A., Artaxo, P., 2003. High aerosol optical depth biomass burning events: A comparison of optical properties for different source regions. Geophys. Res. Lett., 30, 2035, doi:10.1029/2003GL017861, 2003.

Engerer, N.A., Bright, J.M., Killinger, S. 2017. Himawari-8 enabled real-time distributed PV simulations for distribution networks. IEEE-PVSC44 Washington 25th June 2017.

Engerer, N.A., Mills, F.P. 2015. Validating nine clear sky radiation models in Australia. Solar Energy. 120, 9-24.

Gueymard, C.A. 1993. Critical analysis and performance assessment of clear sky solar irradiance models using theoretical and measured data. Solar Energy. 51, 121-138.

Gueymard, C.A. 2008. REST2: High-performance solar radiation model for cloudless-sky irradiance, illuminance, and photosynthetically active radiation – Validation with a benchmark dataset. Solar Energy. 82, 272-285.

Gueymard, C.A., Thevenard, D. 2009. Monthly average clear-sky broadband irradiance database for worldwide solar heat gain and building cooling load calculations. Solar Energy. 83, 1998-2018.

Gueymard, C.A. 2012a. Clear-sky irradiance predictions for solar resource mapping and large-scale applications: improved validation methodology and detailed performance analysis of 18 broadband radiative models. Solar Energy. 86, 2145-2169.

Gueymard, C.A. 2012b. Temporal variability in direct and global irradiance at various time scales as affected by aerosols. Solar Energy. 86, 3544–3553.

Gueymard, C.A. 2014a. Impact of on-site atmospheric water vapor estimation methods on the accuracy of local solar irradiance predictions. Solar Energy. 101, 74-82.

Gueymard, C.A. 2014b. A review of validation methodologies and statistical performance indicators for modeled solar radiation data: Towards a better bankability of solar projects. Renewable and Sustainable Energy Reviews. 39, 1024-1034.

Guia, K., Chea, H., Chenc, Q., Zengd, Z., Liue, H., Wanga, Y., Zhenga, Y., Suna, T., Liaoc, T., Wanga, H., Zhanga, H. 2017. Evaluation of radiosonde, MODIS-NIR-Clear, and AERONET precipitable water vapor using IGS ground-based GPS measurements over China. Atmospheric Research. 197. 461–473.

Hayasaka, T., Satake, S., Shimizu, A., Sugimoto, N., Matsui, I., Aoki, K., Muraji, M. 2007. Vertical distribution and optical properties of aerosols observed over Japan during the Atmospheric Brown Clouds—East Asia Regional Experiment 2005. J. Geophys. Res. 112D. doi:10.1029/2006JD008086.

Holben B.N., Eck, T.F., Slutsker, I., Tanre, D., Buis, J.P., Setzer, A., Vermote, E., Reagan, J.A., Kaufman, Y., Nakajima, T., Lavenu, F., Jankowiak, I., Smirnov, A. 1998. AERONET – A federated instrument network and data archive for aerosol characterization, Rem. Sens. Environ. 66, 1-16.

Ineichen, P. 2016. Validation of models that estimate the clear sky global and beam solar irradiance. Solar Energy. 132, 332-344.

Kang, K., Kumar, R., Hu, K., Yu, X., Yin, Y. 2016. Long-term (2002–2014) evolution and trend in Collection 5.1 Level-2 aerosol products derived from the MODIS and MISR sensors over the Chinese Yangtze River Delta. Atmospheric Research. 181. 29–43.

Kaufman, Y.J., Tanré, D., Remer, L., Vermote, E., Chu, A., Holben, B. 1997. Operational remote sensing of tropospheric aerosols over the land from EOS-MODIS. J. Geophys. Res. 102D, 17051-17061.

Kinne, S. et al. 2003. Monthly averages of aerosol properties: a global comparison among models, satellite data, and AERONET ground data. J. Geophys. Res. 108D. doi:10.1029/2001/JD001253.

Kinne, S. et al. 2006. An AeroCom initial assessment – optical properties in aerosol component modules of global models. Atmos. Chem. Phys. 6, 1815-1834.

Kumar, S., Singh, A.K., Prasad, A.K., Singh, R.P. 2014. Variability of GPS derived water vapor and comparison with MODIS data over the Indo-Gangetic plains. Physics and Chemistry of the Earth 55-57, 11–18.

Kottek, M., Grieser, J., Beck, C., Rudolf, B., Rubel, F., 2006. World map of the Köppen-Geiger climate classifica-

tion updated. Meteorologische Zeitschrift 15, 259–263.

Levy, R.C., Mattoo, S., Sawyer, V., Shi, Y., Colarco, P.R., Lyapustin, A.I., Wang, Y., Remer, L.A. 2018. Exploring systematic offsets between aerosol products from the two MODIS sensors. Atmos. Meas. Tech. 11, 4073-4092.

Liu, J., Liang, H., Sun, Z., Zhoul, X. 2006. Validation of the Moderate-Resolution Imaging Spectroradiometer precipitable water vapor product using measurements from GPS on the Tibetan Plateau. Journal of Geophysical Research. 111. D14103. doi:10.1029/2005JD007028.

Lu, N., Qin, J., Yang, K., Gao, Y., Xu, X., Koike, T. 2011. On the use of GPS measurements for Moderate Resolution Imaging Spectrometer precipitable water vapor evaluation over southern Tibet. Journal of Geophysical Research. 116, D23117, doi:10.1029/2011JD016160.

Pérez-Ramírez, D., Whiteman, D.N., Smirnov, A., Lyamani, H., Holben, B.N., Pinker, R., Andrade, M. and Alados-Arboledas, L. 2014. Evaluation of AERONET precipitable water vapor versus microwave radiometry, GPS, and radiosondes at ARM sites. Journal of Geophysical Research: Atmospheres. 119, 9596-9613.

Prasad, A.K., Singh, R.P. 2009. Validation of MODIS Terra, AIRS, NCEP/DOE AMIP-II Reanalysis-2, and AERONET Sun photometer derived integrated precipitable water vapor using ground-based GPS receivers over India. Journal of Geophysical Research. 114, D05107, doi:10.1029/2008JD011230.

Román, R., Bilbao, J., de Miguel, A. 2014. Uncertainty and variability in satellite-based water vapor column, aerosol optical depth and Angström exponent, and its effect on radiative transfer simulations in the Iberian Peninsula. Atmospheric Environment. 89. 556–569.

Ruiz-Arias, J.A., Dudhia, J., Gueymard, C.A., Pozo-Vázquez, D. 2013. Assessment of the Level-3 MODIS daily aerosol optical depth in the context of surface solar radiation and numerical weather modeling. Atmos. Chem. Phys. 13, 675-692.

Schaap, M. et al. 2008. Evaluation of MODIS aerosol optical thickness over using sun photometer observations. Atmos. Environ. 42, 2187-2197.

Shi, F., Xin, J., Yang, L., Cong, Z., Liu, Z., Ma, Y., Wang, Y., Lu, X., Zhao, L. 2018. The first validation of the precipitable water vapour of multisensory satellites over the typical regions in China. Remote Sensing of Environment. 206, 107-122.

Sinyuk, A., Holben, B.N., Smirnov, A., Eck, T. F., Slutsker, I., Schafer, J.S., Giles, D.M., Sorokin, M. 2012, Assessment of error in aerosol optical depth measured by AERONET due to aerosol forward scattering. Geophys. Res. Lett. 39, L23806, doi:10.1029/2012GL053894.

Sun, X., Wang, P., Gueymard, C.A., Acord, B., Engerer, N.A., Bright, J.M. 2018. Worldwide performance assessment of 57 global clear-sky irradiance models. Solar Energy. In Review.

Vaquero-Martíneza, J., Antón, M., de Galisteo, J.P.O., Cachorro, V.E., Álvarez-Zapatero, P., Román, R., Loyola, D., Costa, M.J., Wang, H., Abad, G.G., Noël, S. 2018. Inter-comparison of integrated water vapor from satellite instruments using reference GPS data at the Iberian Peninsula. Remote Sensing of Environment. 204. 729–740.

Wang, Y., Yang, K., Pan, Z., Qin, J., Chen, D., Lin, C., Chen, Y., Lazhu, Tang, W., Han, M., Lu, N., Wu, H. 2017. Evaluation of Precipitable Water Vapor from Four Satellite Products and Four Reanalysis Datasets against GPS Measurements on the Southern Tibetan Plateau, J. Clim., doi: 10.1175/JCLI-D-16-0630.1.

Wong, M.S., Jin, X., Liu, Z., Nichola, J., Chan, P.W. 2014. Multi-sensors study of precipitable water vapour over mainland China. Int. J. Climatol. doi: 10.1002/joc.4199.

Zhenhong, L., Muller, J.-P., Cross, P. 2003. Comparison of precipitable water vapor derived from radiosonde, GPS, and Moderate-Resolution Imaging Spectroradiometer measurements, Journal of Geophysical Research. 108, D20, 4651. doi:10.1029/2003JD003372.

Zhong, X. and Kleissl, J. 2015. Clear sky irradiances using REST2 and MODIS. Solar Energy. 116. 144-164.